RSC Advances

PAPER

View Article Online
View Journal | View Issue

Cite this: *RSC Adv.*, 2017, **7**, 44712

A statistical physics study of the interaction of [7]-helicene with alkali cations (K^+ and Cs^+): new insights on microscopic adsorption behavior

Mohamed Ben Yahia,[a] Moncef Tounsi,[b] Fatma Aouaini,[a] Salah Knani, *[c] Manel Ben Yahia[d] and Abdelmottaleb Ben Lamine[a]

Received 29th July 2017
Accepted 14th September 2017

DOI: 10.1039/c7ra08387d

rsc.li/rsc-advances

The adsorption of a metal ion to a polycyclic aromatic molecule such as helicene is the object of our study. The latter could function as a chiral molecular clamp for the cationic alkali metal. The main contribution of this work is to attribute new microscopic interpretations for the adsorption of potassium and cesium ions onto a thin layer of helicene achieved by the QCM technique. Throughout the grand canonical ensemble and some theoretical considerations, statistical physics processing has been used for modeling of experimental adsorption isotherms. A new model has been developed and chosen as an appropriate one to present a good correlation with experimental isotherms. Six physico-chemical parameters are obtained from the fitting of the experimental adsorption isotherms. Thanks to the steric parameters, we have found that an increase in temperature promotes a rise in the numbers of ions per site n_1 and n_2 and raises the adsorption capacities N_{M1} and N_{M2}. The two energetic parameters c_1 and c_2 allow deduction of the adsorption energies at four temperatures. It is found from the calculated energies that physical adsorption takes place; the helicene can function as potassium and cesium captor and the K^+–helicene complex is more stable than the Cs^+–helicene complex.

1. Introduction

Helicenes are polycyclic aromatic compounds consisting of ortho-fused benzene rings with nonplanar topology with C_2-symmetric axis perpendicular to the axis of helicity as a result of the steric repulsive interaction between terminal aromatic rings.[1–3] This makes them chiral even though they have no center of chirality. The highly delocalized large π-electron system of fully aromatic helicenes along with the previously mentioned inherent chirality predetermines their unique optical[4] and electronic[5] properties, as well as their use in many fields of research including supramolecular chemistry,[6–9] molecular recognition,[10,11] and asymmetric organo- or transition metal catalysis.[12,13]

[7]-Helicene (Fig. 1a) is a particularly interesting member of the carbohelicene family. Seven contiguous benzenoid rings give rise to a scaffold that completes one full turn of the helix (Fig. 1b). Furthermore, the two terminal rings of this helicene are co-facial (Fig. 1c).

It was apparent to us that such a structure provides a central cavity that could potentially host a suitably sized guest, with the co-facial terminal rings providing a stabilizing interaction. In this respect [7]-helicene would be functioning as a "molecular tweezer",[14,15] a term coined by Whitlock[16] to describe a simple molecular receptor characterized by two flat, generally aromatic pincers, separated by some kind of tether, which is more or less rigid.[16] Indeed, many recent studies have emerged the possibility of [7]-helicene acting as a molecular tweezer of alkali metal cations (Li^+, Na^+, K^+, Cs^+), and transition metals (Cr, Mo, W).[17]

In recent years, several experimental and theoretical studies have been carried out on helicenes and related molecules including the determination of their racemization barriers,[18,19] aromatic character[20] and nonlinear optical properties (*e.g.* of tetrathia-helicenes). However, interactions between helicenes and atoms/ions as well as other molecules do not appear to have been studied. This is attempted in the present investigations.

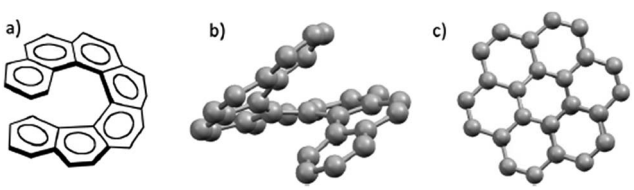

Fig. 1 Hepta-helicene: (a) skeletal image; (b) as viewed from the side; (c) as viewed from above.

[a]*Research Unit of Quantum Physics 11 ES 54, Faculty of Sciences of Monastir, Tunisia. E-mail: abdelmottaleb.benlamine@gmail.com*

[b]*Interfaces Laboratory and Advanced Materials, (LIMA), Faculty of Sciences of Monastir, Tunisia*

[c]*Northern Border University, College of Science, Arar, P.O. Box 1631, Saudi Arabia*

[d]*Department of Physics, Faculty of Science, King AbdulAziz University, Rabigh, Saudi Arabia. E-mail: knanisalah@yhoo.fr; Tel: +966 500886582; +216 95666600.*

We were therefore keen to investigate the experimental possibility of [7]-helicene functioning as a chiral molecular tweezer of metallic cations (K^+ and Cs^+).

Our study is essentially based on two parts: in the first we detailed the experimental method used to obtain the adsorption isotherms of potassium and cesium onto thin layer of hepta-helicenes at four temperatures. Secondly, throughout the statistical physics formalism, we will propose a new theoretical model which presents a high correlation with the experimental curves to interpret the adsorption processes.

2. Materials and methods

2.1. Adsorbent

The adsorbent used is the hepta-helicene: Fig. 2 shows the reason why [7]-helicene ($C_{30}H_{18}$) alone has been chosen for the present work.

The profile of the molecule shows the two terminal overlapping benzene rings in the form of a crocodile's jaws. Other helicenes do not have such a profile. Therefore, it would be worthwhile to investigate the nature of the interactions of [7]-helicene with cations of alkali metals. In other words, how do the ions and molecules slide into the 'jaws' of [7]-helicene and how do the 'jaws' open up to receive the 'food'? Such an interaction might also be able to model, *e.g.* drug-DNA interactions. It has long been known through crystallographic studies of the DNA–actinomycin D interacting system[21] that as the drug slides into DNA, DNA first opens up to receive the incoming molecule and then 'bites down' on it through stretching, bending, sliding and unwinding motions of the sugar-phosphate backbone *via* the corresponding normal modes. For [7]-helicene to mimic such interactions, it would be of interest to see whether this relatively smaller molecule has adequate flexibility in its backbone in the case of its interaction with alkali metals.

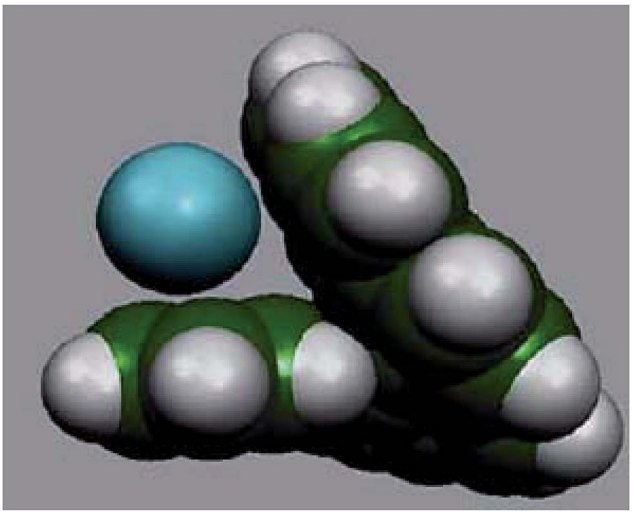

Fig. 2 Profile of [7]-helicene seemingly trying to 'devour' an Alkali metal.

2.2. Adsorbates

The adsorbates used are the potassium chloride and the cesium chloride:

Cesium chloride is the inorganic compound with the formula CsCl. This colorless solid is an important source of cesium ions in many applications. Cesium chloride dissolves in water.

Potassium chloride (KCl) is a metal halide salt composed of potassium and chloride. It is odorless and has a white or colorless vitreous crystal appearance. The solid dissolves readily in water and its solutions have a salt-like taste. KCl is used in medicine and many other scientific applications.

The ultimate goal of this study was to explore the adsorption phenomenon of alkali metal on a solid surface. The quartz crystal microbalance (QCM) technique may be a comparatively good and effective method for the monitoring of helicene adsorption. The QCM method has been successfully used for the investigation of the adsorption process at the solid–solution interface.[22,23]

2.3. Adsorption experiments

The experimental setup for the adsorption measurements with the quartz crystal microbalance is depicted in Fig. 3. The QCM[24–26] setup consisted of the coated electrode, the QCM instrument, a crystal holder, and adsorption cell.

For film deposition, a volume of 30 μL of hepta-helicenes was spin coated at 3000 rpm for 1 min onto the larger gold electrode to cover the overlapping electrodes portion (Fig. 4). The coated crystals were then dried at 100 °C for at least 2 h.

After drying, we started our measurements. The QCM crystal holder was immersed in the adsorption cell filled with V_s = 100 mL of pure water. After stabilization of the QCM frequency change, 100 μL of the prepared stock solution of KCl or CsCl was injected and stirred with a magnetic stirrer; one hour was found to be enough to reach adsorption equilibrium. The detection signals and calculated adsorbed mass in the conventional QCM are solely based on the assumption that the changes of the fundamental piezoelectric frequency is proportional to the

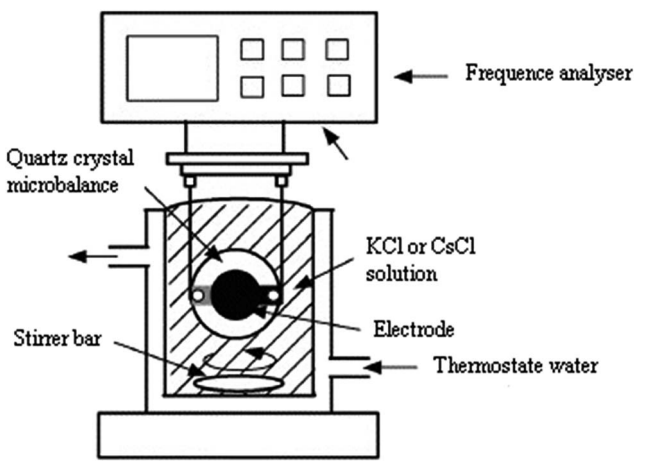

Fig. 3 Experimental setup for adsorption measurements with QCM.

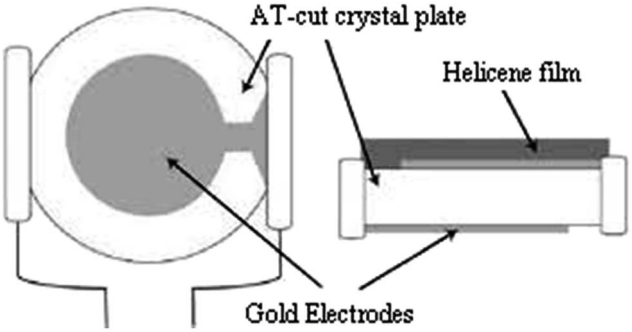

Fig. 4 Helicene coated onto quartz crystal.

change of adsorbed mass on the surface of the quartz crystal calculated from the classical Sauerbrey equation:[27]

$$\Delta F = -\frac{2F_0^2}{A\sqrt{\rho\mu}}\Delta m \quad (1)$$

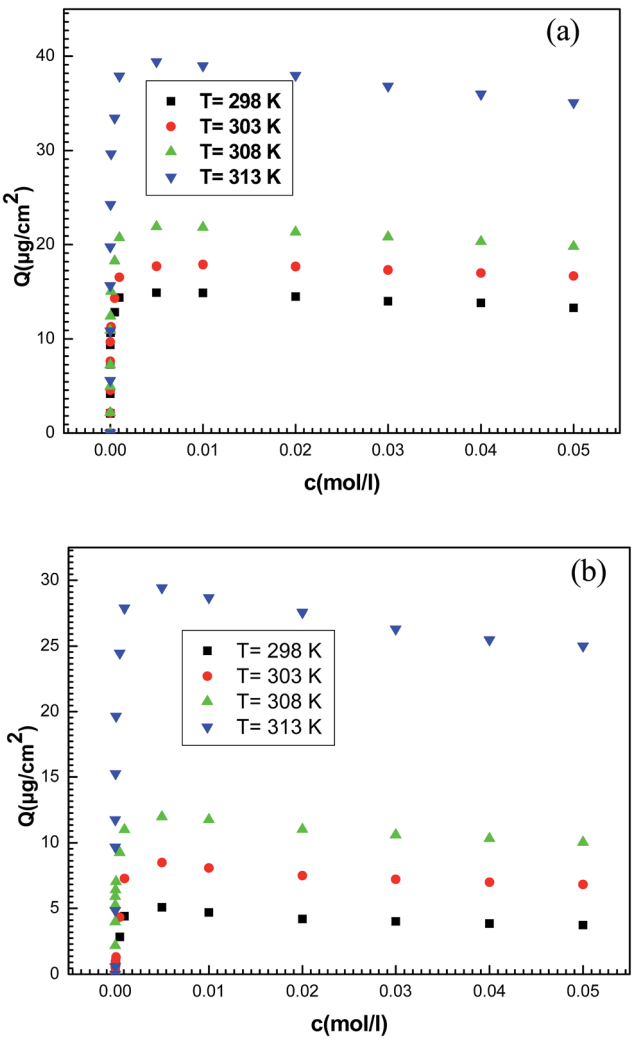

Fig. 5 Experimental adsorption isotherms of (a) potassium chloride and (b) cesium chloride on a thin layer of hepta-helicenes for the four temperatures.

where ΔF is the frequency shift (Hz), F_0 is the resonant frequency of the crystal (Hz), Δm is the adsorbed amount (μg), A is the active electrode area (cm^2), ρ is the density of quartz (2.648 g cm^{-3}), and μ is the shear modulus of quartz (2.947×10^{11} g cm^{-1} s^{-2}).

Thus, the constant terms can be combined together to give a crystal sensitivity constant, C, which is specific to crystal:[28]

$$\Delta m = -\frac{\Delta F_m}{C} \quad (2)$$

where $C = 56.6$ μg^{-1} cm^2 Hz for a 5 MHz AT-cut quartz crystal. The resonant frequency of a 5 MHz quartz crystal can be measured with a precision of about 0.01 Hz in vacuum and 0.1 Hz in liquids. Accordingly, very small masses on the nanogram and microgram scales could be measured by the QCM.

The adsorbed amount of potassium and cesium ions per unit of area expressed in μg cm^{-2} is conducted directly from the measured frequency after each injection (Fig. 5).

In the following we use a statistical physics treatment to establish the expression of statistical model giving the adsorbed quantity *versus* the concentration. Secondly we apply the adequate analytical expression to fit experimental isotherms.

3. Theory

Measurement and modeling of adsorption isotherms has attracted numerous researchers because of their application in industrial practice. Numerous mathematical models for the description of adsorption isotherms are available in the literature. Some of these models are based on theories of the adsorption mechanism; others have been purely empirical, or semi-empirical. It is difficult to have a unique mathematical model whether theoretical or empirical that describes accurately the adsorption isotherm. The criteria used to select the most appropriate adsorption model were the degree of fit to the experimental data and the simplicity of the interpretation of the model. In our theoretical development, we rely on a statistical physics treatment and some assumptions will be considered to simplify the theoretical calculations. This theoretical base will allow us to better interpret and to deduce information about adsorption process at the microscopic scale.

Adsorption involves an exchange of particles from free state to the adsorbed one. Its investigation cannot be performed without employing the grand canonical ensemble to take into account the particle number variation through the introduction of a variable chemical potential μ in the adsorption process. Although the overall system is canonical, the canonical ensemble and the grand canonical one are considered equivalent as it is a macroscopic system. The fluctuations may be neglected as the system is at the thermodynamic limit. Therefore the system can be studied using the grand canonical ensemble with the results being interpreted canonically.[29]

It is also assumed that the internal degree of freedom of the adsorbate ions may be neglected in aqueous solution there by allowing only the most important degree of freedom, *i.e.* the translational one, to be taken into account. This arises because the electronic degree of freedom cannot be excited thermally

and the rotational degree of freedom is hampered in solution. The vibrational degree of freedom can be neglected in comparison with the translational one.

According to these assumptions, in liquid phase, the adsorption reaction of liquid ions (A) onto receptor sites (S) should include a stoichiometric coefficient n as shown in the following equation:

$$nA + S \leftrightarrows A_nS \tag{3}$$

where n represents the number of adsorbed ions per site A and A_nS is the formed metal–helicene complex.[30,31]

The grand canonical partition function in this case, for only one site, has the form:

$$z_{gc} = \sum_{N_i} e^{-\beta(-\varepsilon_i-\mu)N_i} \tag{4}$$

where N_i is the state of occupation number, β is the Boltzmann factor, $(-\varepsilon_i)$ is the receptor site adsorption energy and μ is the chemical potential. The total grand canonical partition function related to N_M receptor sites per surface unit, which is assumed to be independent and identical, is written as:[32]

$$Z_{gc} = (z_{gc}(T,\mu))^{N_M} \tag{5}$$

The occupation number for N_M identical receptor sites is therefore given as follow:[33]

$$N_o = N_M k_B T \frac{\partial \ln(z_{gc})}{\partial \mu} \tag{6}$$

The adsorbed quantity (Q) is given per unit surface, because the density of receptor sites (N_M) is written per unit surface and is written as:[34,35]

$$Q = nN_o \tag{7}$$

Finally, to get any model expression, it is sufficient to write the adequate grand canonical partition function and follow the last steps (eqn (4)–(7)). The use of statistical physics principles will allow, firstly, establishing the model expressions and secondly, to better interpret and deduce information about adsorption process at a molecular level, which could not be achieved by means of empirical models.

There are many theories relating to adsorption equilibrium. So, three models are proposed: monolayer, double layer and finite multilayer models. For the first model, there are three fitting parameters, for the second, it is assumed that each receptor site can be empty or occupied once or twice whereas for the third model we assumed that L_1 layers of adsorbed ions are formed one after the other with the first energy $(-\varepsilon_1)$ and L_2 layers with the energy $(-\varepsilon_2)$.

The equations of these models and their corresponding grand canonical partition functions are summarized in Table 1.

With A, B and C are functions of the concentration such as:

$$A = \frac{-X_1{}^{(L_1+1)}(L_1+1)}{1-X_1} + \frac{X_1\left(1-X_1{}^{(L_1+1)}\right)}{(1-X_1)^2} \tag{11}$$

$$B = \frac{X_1{}^{L_1}X_2(L_1+1)\left(1-X_2{}^{L_2}\right)}{1-X_2} - \frac{X_1{}^{L_1}X_2{}^{(1+L_2)}L_2}{1-X_2} + \frac{X_1{}^{L_1}X_2{}^2\left(1-X_2{}^{L_2}\right)}{(1-X_1)^2} \tag{12}$$

$$C = \frac{\left(1-X_1{}^{(L_1+1)}\right)}{1-X_1} + \frac{X_1{}^{L_1}X_2\left(1-X_2{}^{L_2}\right)}{1-X_2} \tag{13}$$

where: $X_1 = \left(\frac{c}{c_1}\right)^n$ and $X_2 = \left(\frac{c}{c_2}\right)^n$.

In the expression of adsorbed quantity given by each model there are two classes of parameters, the first is a steric aspect such as the number of ions per site n, the density of receptor sites N_M, and the two average number of adsorbed layers L_1 and L_2, the second aspect is energetic one given by the parameters c_1 and c_2 which are function of the adsorption energies.

$$c_1 = c_s e^{-\frac{\Delta E_1{}^a}{RT}} \tag{14}$$

$$c_2 = c_s e^{-\frac{\Delta E_2{}^a}{RT}} \tag{15}$$

with $(-\Delta E_1{}^a)$ and $(-\Delta E_2{}^a)$ are the molar adsorption energies, c_s is the solubility of adsorbate in aqueous solution and R (8.314 J K^{-1} mol^{-1}) is the ideal gas constant.

We note that our experimental data present a decreasing in the adsorbed quantity after saturation. So in the next step, we will prove that these three statistical models can't describe the adsorption isotherms of potassium and cesium on hepta-helicene.

3.1. Fitting results

Our objective is to select the adequate model, which presents a high correlation with the experimental curves. To fit these adsorption isotherms, computational software was applied based on the Levenberg–Marquardt iterating algorithm using a multivariable non-linear regression.

The figure of merit used as indicator of the overall goodness-of-fit of the model to the data is the multiple correlation coefficients squared, R^2 also known as the coefficient of determination which is a standardized measure of the goodness-of-fit. This coefficient is given by:[36]

$$R^2 = 1 - \left[\left(1 - \frac{\sum_i^{n_p}\left(Q_{i,exp} - \overline{Q}_{i,exp}\right)^2 - \sum_i^{n_p}\left(Q_{i,exp} - Q_{i,model}\right)^2}{\sum_i^{n_p}\left(Q_{i,exp} - \overline{Q}_{i,exp}\right)^2}\right) \times \left(\frac{n_p - 1}{n_p - p}\right)\right] \tag{16}$$

where $Q_{i,model}$ is each value of Q predicted by the fitted model, $Q_{i,exp}$ is each value of Q measured experimentally, $\bar{Q}_{i,exp}$ is the average of Q experimentally measured, n_p is the number of experiments performed and p is the number of parameters of the fitted model.

Table 1 Analytical expressions of the three models and their corresponding grand canonical partition functions

Statistical model	Partition function	Adsorbed quantity
Mono-layer	$z_{gc} = 1 + e^{\beta(\varepsilon+\mu)}$	$Q = nN_0 = \frac{nN_M}{1+\left(\frac{c_1}{c}\right)^n}$ (8)
Double-layer	$z_{gc} = 1 + e^{\beta(\varepsilon_1+\mu)} + e^{\beta(\varepsilon_1+\varepsilon_2+2\mu)}$	$Q = nN_M \frac{\left(\frac{c}{c_1}\right)^n + 2\left(\frac{c}{c_2}\right)^{2n}}{1+\left(\frac{c}{c_1}\right)^n + \left(\frac{c}{c_2}\right)^{2n}}$ (9)
Multi-layer	$z_{gc} = \sum_{N_i=0}^{L_1} e^{-\beta(-\varepsilon_1-\mu)N_i} + \sum_{N_i=L_1+1}^{L_2} e^{-\beta(-L_1\varepsilon_1-N_i\varepsilon_2-(N_i+L_1)\mu)N_i}$	$Q = \frac{nN_M(A+B(c,c_1,c_2))}{C(c,c_1,c_2)}$ (10)

The choice of the ideal fitting model is based on two criteria: the first one is obtained when the value of R^2 is close to the unit and the best fitting result is established once the residuals between the experimental data and adsorbed quantities value predicted by the model are minimized according to a determined level of confidence. In our case, the level of confidence was set at 95%. The second is that the parameters are acceptable and can facilitate and enrich the interpretation of the adsorption process.

In Tables 2 and 3 we present the R^2 values deduced from the fit of the experimental adsorption isotherms of the potassium and cesium onto helicenes.

We noticed that the values of adjustment coefficients R^2 given by these models vary from 0.68 to 0.89. These fitting values don't reach the level of confidence. So, we conclude that the adsorption of potassium and cesium ions cannot be explained by these models.

In comparison between the three models we note that the monolayer model presents the best values of R^2 which traduce a physical reason that the adsorption cannot exceed one layer. Nevertheless, this model cannot fit the adsorption isotherms with good approximation.

The principal motivation to find another model is that the adsorption isotherms present a decrease of adsorbed quantity *versus* concentration such behavior cannot be explained by the three previous models. Therefore, a new model will be developed throughout the processing statistical physics and we will show that the proposed model is sufficiently flexible to give a good representation of the experimental data.

3.2. New theoretical development

In order to develop the expression of this model, a variable number of potassium or cesium ion are hypothesized to be adsorbed onto two different adsorption sites having different energy level. The number of sites of the first type is N_{M1} sites per unit of surface and the number of the second type is N_{M2}. We suppose that the adsorption onto the first type is carried out with the energy $(-\varepsilon_1)$ and onto the second type with the energy $(-\varepsilon_2)$. We define the state of occupation N_i and it is assumed that any given receptor site can either be empty, and consequently N_i takes the value 0, or occupied so N_i is equal to the unit. In this case, we can write the grand canonical partition function for each type of receptor site:

$$z_{1gc} = 1 + e^{\beta(\varepsilon_1+\mu_1)} \quad (17)$$

$$z_{2gc} = 1 + e^{\beta(\varepsilon_2+\mu_2)} \quad (18)$$

where z_{1gc}, z_{2gc} are the partition functions of the two types of sites, μ_1 and μ_2 being the chemical potential of adsorbed ions in different types of sites.

The total grand canonical partition function has the following form:

$$Z_{gc} = (z_{1gc})^{N_{M1}}(z_{2gc})^{N_{M2}} \quad (19)$$

The choice of two energies levels is not arbitrary but based on physical reasons. The first is based on work elaborated by Tan *et al.*[43] which suggest that the helicene might be open its two terminal overlapping benzene rings to form a crocodile's jaws able to attract the alkali cations. The second one is that the helicene molecule presents aromatic cycles and for electrostatic reason can probably attract the ions.

Using the same treatment elaborated by Nakhli *et al.*,[37] the adsorbed quantity *versus* concentration is written as:

$$Q = \frac{n_1 N_{M1}}{1+\left(\frac{c_1}{c}\right)^{n_1}} + \frac{n_2 N_{M2}}{1+\left(\frac{c_2}{c}\right)^{n_2}} \quad (20)$$

where c_1 and c_2 are two energetic parameters which can be written as:

Table 2 Values of R^2 of fitting potassium chloride–helicene by mono-layer, double-layer and multi-layer models

T (K)	298	303	308	313
Mono-layer	0.69711	0.69795	0.89763	0.79476
Double-layer	0.87541	0.78373	0.67149	0.78792
Multi-layer	0.79832	0.89806	0.79804	0.79779

Table 3 Values of R^2 of fitting cesium chloride–helicene by mono-layer, double-layer and multi-layer models

T (K)	298	303	308	313
Mono-layer	0.89711	0.79795	0.79763	0.89476
Double-layer	0.87541	0.68373	0.77149	0.88792
Multi-layer	0.79832	0.69806	0.69804	0.86779

$$c_1 = w_1(1 - bc)e^{2\beta ac}e^{-\frac{bc}{1-bc}} \quad (21)$$

$$c_1 = w_2(1 - bc)e^{2\beta ac}e^{-\frac{bc}{1-bc}} \quad (22)$$

with a and b being two parameters reproducing the interaction between the adsorbate during the adsorption process. The coefficients w_1 and w_2 are written as function of the energies of adsorption.

$$w_1 = c_s e^{-\frac{\Delta E_1{}^a}{RT}} \quad (23)$$

$$w_2 = c_s e^{-\frac{\Delta E_2{}^a}{RT}} \quad (24)$$

with c_s is the solubility of adsorbate in aqueous solution, R is the ideal gas constant and T is the isotherm temperature. $(-\Delta E_1{}^a)$ and $(-\Delta E_2{}^a)$ are the adsorption energies at the first type of site and the second one, respectively.

Finally, using the equilibrium condition and the previous definition given by eqn (7) the adsorbed quantity *versus* concentration is given by the following expression:

The expression of this model giving the adsorbed quantity *versus* concentration involves six physicochemical parameters. The parameters numbers of ions per site (n_1 and n_2) imply that the receptor site can be either empty or occupied by one or more potassium or cesium ion. The N_{M1} and N_{M2}, density of receptor sites, give information about partial saturation when the totality of type of sites is occupied. c_1 and c_2 are two energetic parameters.

The proposed model will be simulated to the experimental adsorption isotherm.

In Table 4 we present the R^2 values deduced from the fit of the experimental adsorption isotherms of the potassium chloride and cesium chloride to helicene.

In Fig. 6 we illustrate the fit of adsorption isotherms at four temperatures by new model.

We noticed that our model presents the high R^2 values in comparison with the three previous models. These values vary from 0.995 to 0.998 and the fitting parameters are acceptable physically. So, we conclude that, using a statistical physics treatment, the proposed model is sufficiently flexible to give a good representation of the experimental data and it is able to predict some information about the adsorption of the alkali metals onto the adsorbent surface.

In the next section, we will investigate the effect of each parameter on the adsorbed quantity *versus* the adsorbate concentration.

3.3. Physical interpretations of the model parameters

To better understand the physical significance of the six physico-chemical parameters: n_1, n_2, N_{M1}, N_{M2}, c_1 and c_2 of the new model with two energy levels, the effect of each parameter on the adsorption isotherms of potassium and cesium onto hepta-helicene will be investigated.

Table 4 Values of coefficient of determination R^2 of fitting by the new model

Isotherms	$T = 298$ K	$T = 303$ K	$T = 308$ K	$T = 313$ K
Potassium–helicene	0.996	0.995	0.998	0.997
Cesium–helicene	0.997	0.998	0.997	0.996

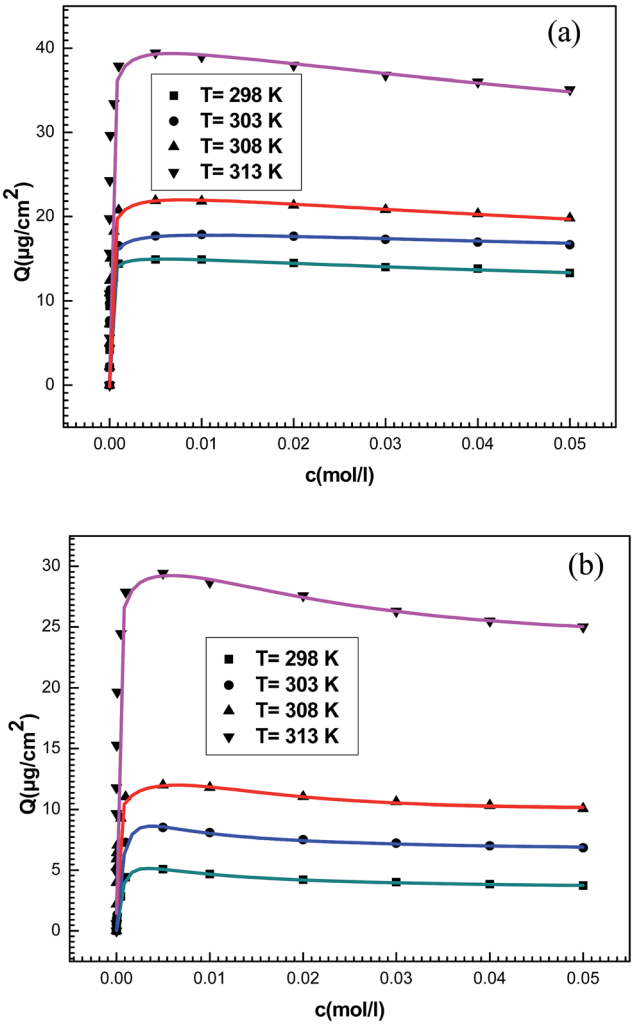

Fig. 6 Experimental data of adsorption isotherms of (a) potassium and (b) cesium fitted by statistical model (illustrated by different lines at different colors) at different temperatures.

3.3.1. Effect of n_1 and n_2. The parameter n_1 and n_2 are stoichiometric coefficients in the adsorption process. As proposed by Knani *et al.*,[38] these numbers also convey the anchorage manner of the adsorbate onto the adsorbent and they can be greater or smaller than 1.

The effect of such steric parameters on the adsorption process may be understood from Fig. 7 where the relationship between the adsorbed quantity and the adsorbate concentration is plotted for four values of n_1 and n_2. We can note that the number of ions per site n_1 and n_2 are relevant in the behavior of the isotherm. Indeed, the greater the value of n_1 and n_2, the greater is the adsorbed quantity for both systems. We can also notice that the parameter n_1 acts on the first part of the isotherm until saturation, and then the parameter n_2 is manifested beyond the first partial saturation due to energetic consideration. In fact, the receptor sites that have the stronger

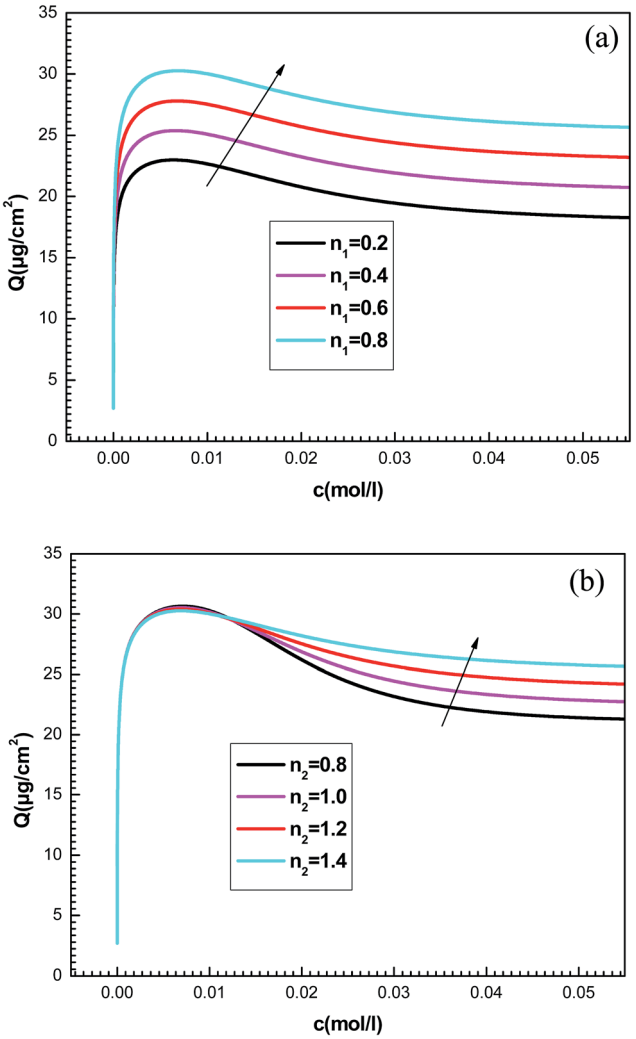

Fig. 7 Influence of parameters n_1 (a) and n_2 (b) on the shapes of adsorption isotherms generated by the statistical model.

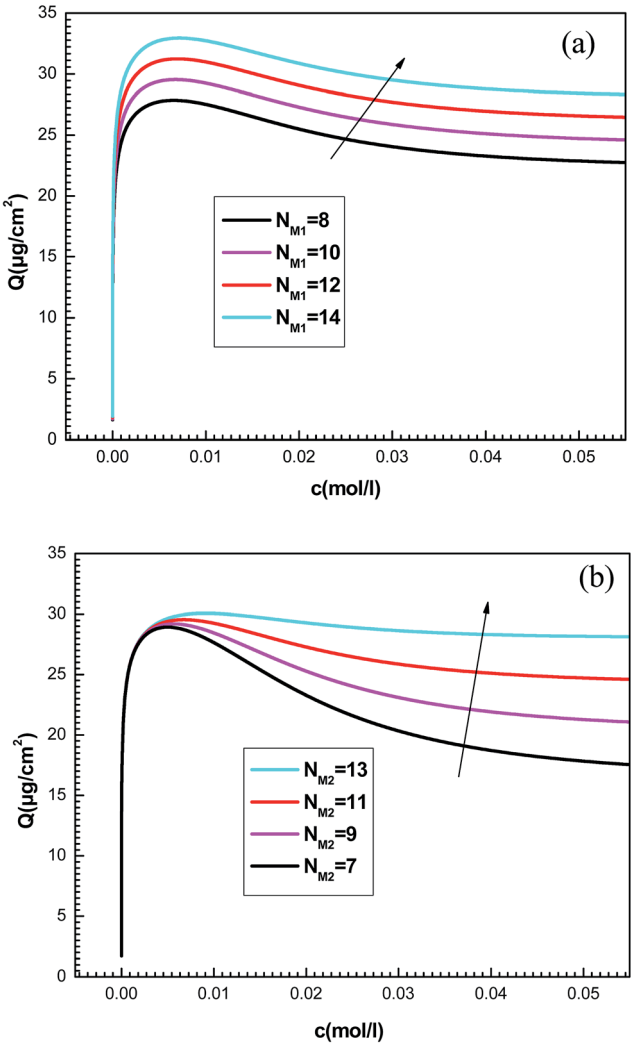

Fig. 8 Influence of the number of the density of receptor sites N_{M1} (a) and N_{M2} (b) on the plots of adsorption isotherms.

energy will be rapidly and easily occupied. However, at low concentrations, only the first-type receptor sites are occupied. Then the number of ions per site n_2 intervenes after the first partial saturation, which is relevant at high concentration when the totality of receptor sites is occupied.

3.3.2. Effect of N_{M1} and N_{M2}. The influence of N_{M1} and N_{M2} on the adsorbed quantity is reported in Fig. 8.

The quantities N_{M1} and N_{M2} are parameters associated with the number of receptor sites and, thus, a steric coefficients. These constants are responsible for the receptor sites accessible to adsorbate ions. We can notice that the influence of $N_{Mi(i=1,\ 2)}$ is similar as that observed for $n_{i(i=1,\ 2)}$ because these four constants are steric parameters related to the monolayer formation. It can also be noted that the increase of N_{M1} and N_{M2} values is followed by the rise of the adsorbed quantity. This is due to the high probability of finding a sufficient number of empty sites to be occupied by the adsorbates.

3.3.3. Effect of energetic parameters c_1 and c_2. These parameters appear as energetic coefficients governing the dynamics of the adsorption process. It should also be noted that c_1 and c_2 are coefficients that contain the temperature effect; this is arising from the Boltzmann factor and from the partition function. The effect of c_1 and c_2 on the adsorption isotherm is shown in Fig. 9.

We notice that c_1 is the concentration at half-saturation which changes the shape of isotherms at low concentrations and c_2 is the concentration at half saturation which intervenes at high concentration. By increasing c_1, we notice that the adsorption is delayed with concentration. The greater the value of c_1 is, the lower the adsorbed amount becomes. Also the rise in the value of the constant c_2 decreases the adsorbed quantity at high concentrations. A simple question can arise regarding the physical meaning of c_1 and c_2 and why they govern the dynamics of adsorption.

This can be easily understood if we observe that both c_1 and c_2 are functions of the specific adsorption energies $(-\Delta E_1{}^a)$ and $(-\Delta E_2{}^a)$ (kJ mol^{-1}) of the ions on receptor sites which are stated in the expressions (14) and (15). c_1 increases as adsorption energy increases algebraically (decreases in module). Therefore,

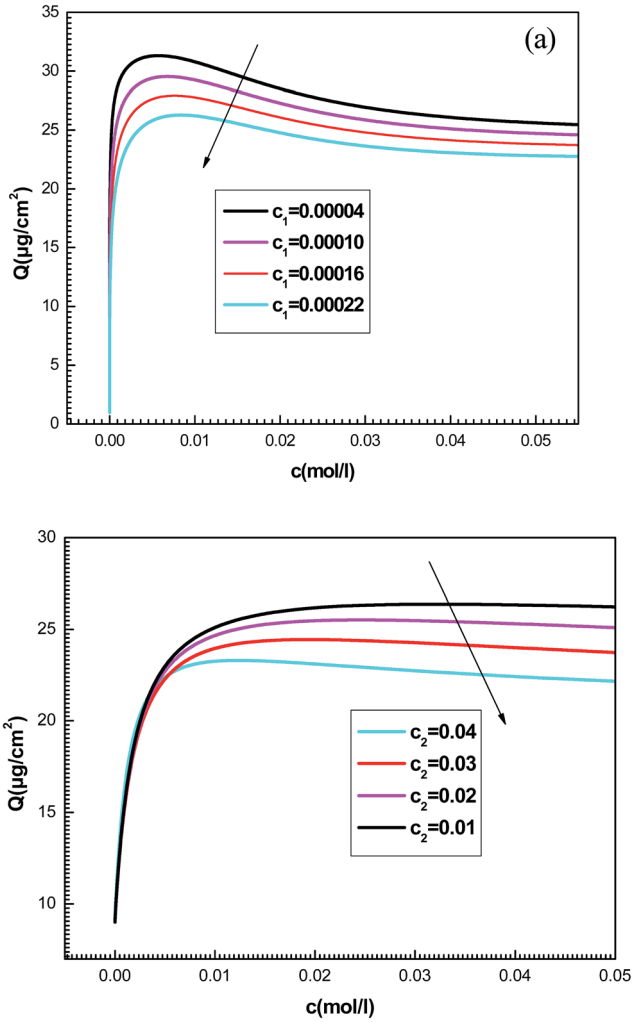

Fig. 9 Effect of concentrations at half-saturation c_1 (a) and c_2 (b) on the shapes of adsorption isotherms given by the new model.

at large values of c_1 and c_2 that correspond to low energies values in module, *i.e.* a low binding energy, the adsorption is reduced. Therefore, we can conclude that the receptor sites that have the stronger energy will be rapidly occupied and the adsorbed amount becomes more important.

The different parameter values of the fitted adsorption isotherms of K^+ and Cs^+ ions and their evolutions *versus* temperature will be interpreted in the following section.

4. Microscopic study of adsorption processes

The parameters deduced from the fitting of the experimental adsorption isotherms by numerical simulation are presented in Table 5.

4.1. Steric interpretations

4.1.1. Numbers of ions per site n_1 and n_2. From Table 5 one can note that all values of n_1 are smaller than 1 for both systems. As proposed by Knani *et al.*[38,39] this number $n_{i(i=1,\ 2)}$ can be either superior or inferior to 1. For n superior to 1, this parameter represents the number of particles per site *i.e.* one site can be occupied by more than 1 ion. For the case n_i inferior to 1 a fraction of ion is adsorbed which imply that one ion is adsorbed on more than 1 site. So, $1/n_i$ is the anchorage number which represents the number of sites occupied by one ion. The number of ions per site can be also written as percentage of two types of anchorage. For example, for the adsorption of K^+ at 298 K, n_1 is equal to 0.76, this value can be written as the weighted average between 1/2 and 1, giving a number of anchorages n' varying between 1 and 2. The value of n_1 represents an average between two types of K^+ ions having one anchorage ($n_1' = 1$) and two anchorages ($n_2' = 2$). If x denote the percentage of ions with a single anchorage, the percentage of ions having two anchorages is then $(1 - x)$. Therefore one can write: $0.76 = x \times 1 + (1 - x) \times 0.5$, which rules out that 52% of K^+ ions are anchored with a single anchorage and 48% of K^+ ions were also anchored with two sites, indicating multi-anchorage adsorption.

Concerning the number of adsorbed ions per site n_2, they are always greater than the unit for both systems at the four temperatures. So, two adsorbate ions can be gathered in solution forming a kind of aggregate and can be anchored on one site.

n_2 is normally an integer but its fitted values are not, since they are an average of some successive integer values. For example, the value of n_2 is equal to 1.02 for the adsorption of K^+ at 298 K. In the same way n_2 can be deduced as average value between two successive integers 1 and 2. This means that the receptor site will be occupied by one or two ions with the respective percentages x and $(1 - x)$. Then, we can write: $1.02 = 1 \times x + (1 - x) \times 2$ which gives a rate of 98% of receptor sites are occupied by one ion and 2% of receptor sites are occupied by two ions indicating that no aggregation occurred prior and during the adsorption process. This is simply due to the repulsive electrostatic positive charge of adsorbate ions K^+ and Cs^+.

The variation *versus* temperature of the numbers of ions per sites n_1 and n_2 is reported in Fig. 10. It is shown that the numbers of adsorbed ions n_1 and n_2 for the studied systems increased with the temperature. This is due to the thermal agitation effect.

4.1.2. Densities of receptor sites N_{M1} and N_{M2}. These steric parameters N_{M1} and N_{M2} give information about the numbers of receptor sites accessible to the adsorbed ions. They also described the occupied receptor sites per unit surface when the saturation point is reached.

The densities N_{M1} and N_{M2} notably increase (Fig. 11) *versus* temperature for both systems. Indeed, these densities for each ion are relatively similar to the corresponding n_1 and n_2. So, it can be noted that the increase in temperature allow the formation of supplementary active sites that are hidden at low temperatures due probably to energetic reasons which leads to an increase in the amount of adsorbed ions.

However, it is not possible to predict what kind of chemical or physical binding of the molecule with the receptor sites. Nevertheless, from the binding energy, *i.e.*, adsorption energies $(-\Delta E_1^a)$ and $(-\Delta E_2^a)$ we can propose some different cases, which are plausible with the numerical values.

Table 5 Values of adjustment parameters corresponding to the fitting with statistical model of the potassium on helicenes (systems (a)) and cesium on helicenes (systems (b))

Isotherms	$T = 298$ K	$T = 303$ K	$T = 308$ K	$T = 313$ K
System (a): potassium–helicenes	$n_1 = 0.76723$	$n_1 = 0.85923$	$n_1 = 0.89974$	$n_1 = 0.98655$
	$n_2 = 1.02397$	$n_2 = 1.04551$	$n_2 = 1.07407$	$n_2 = 1.08035$
	$N_{M1} = 12.20231$	$N_{M1} = 13.63313$	$N_{M1} = 14.73793$	$N_{M1} = 17.04737$
	$N_{M2} = 11.9603$	$N_{M2} = 12.07024$	$N_{M2} = 13.32572$	$N_{M2} = 16.42445$
	$w_1 = 0.00002$	$w_1 = 0.00003$	$w_1 = 0.00004$	$w_1 = 0.00006$
	$w_2 = 0.0002$	$w_2 = 0.00015$	$w_2 = 0.005$	$w_2 = 0.006$
	$c_1 = 0.0002$	$c_1 = 0.00025$	$c_1 = 0.00027$	$c_1 = 0.00028$
	$c_2 = 0.01008$	$c_2 = 0.01652$	$c_2 = 0.01379$	$c_2 = 0.01546$
System (b): cesium–helicenes	$n_1 = 0.61511$	$n_1 = 0.73827$	$n_1 = 0.86247$	$n_1 = 0.88247$
	$n_2 = 1.00164$	$n_2 = 1.03456$	$n_2 = 1.06478$	$n_2 = 1.09813$
	$N_{M1} = 8.12675$	$N_{M1} = 10.31894$	$N_{M1} = 11.85264$	$N_{M1} = 13.09462$
	$N_{M2} = 7.21648$	$N_{M2} = 10.31587$	$N_{M2} = 12.31584$	$N_{M2} = 14.9998$
	$w_1 = 0.00003$	$w_1 = 0.00004$	$w_1 = 0.00005$	$w_1 = 0.0006$
	$w_2 = 0.001$	$w_2 = 0.003$	$w_2 = 0.00041$	$w_2 = 0.005$
	$c_1 = 0.00301$	$c_1 = 0.00336$	$c_1 = 0.00302$	$c_1 = 0.00265$
	$c_2 = 0.07587$	$c_2 = 0.06324$	$c_2 = 0.06989$	$c_2 = 0.07994$

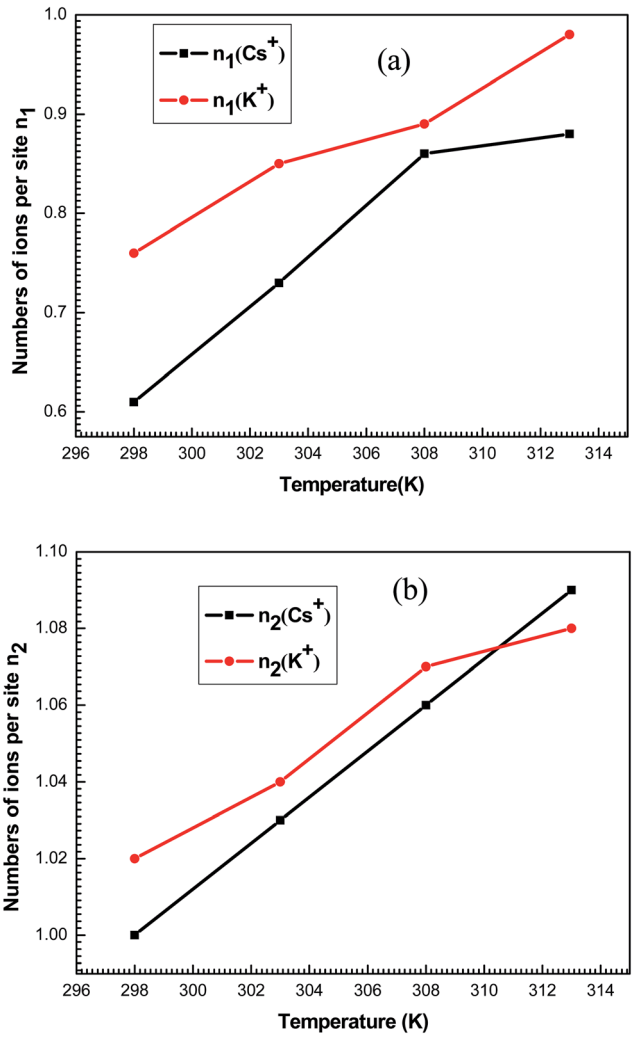

Fig. 10 Evolution of the numbers of ions per site n_1 (a) and n_2 (b) for K^+ and Cs^+ as a function of temperature.

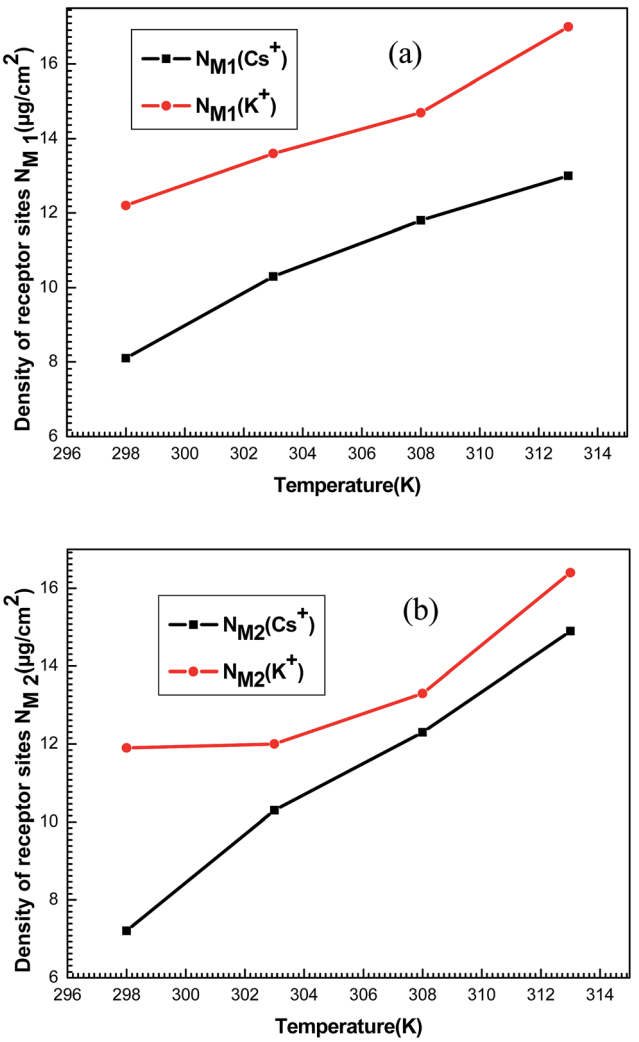

Fig. 11 Evolution of the densities of receptor sites N_{M1} (a) and N_{M2} (b) of potassium and cesium in function of temperature.

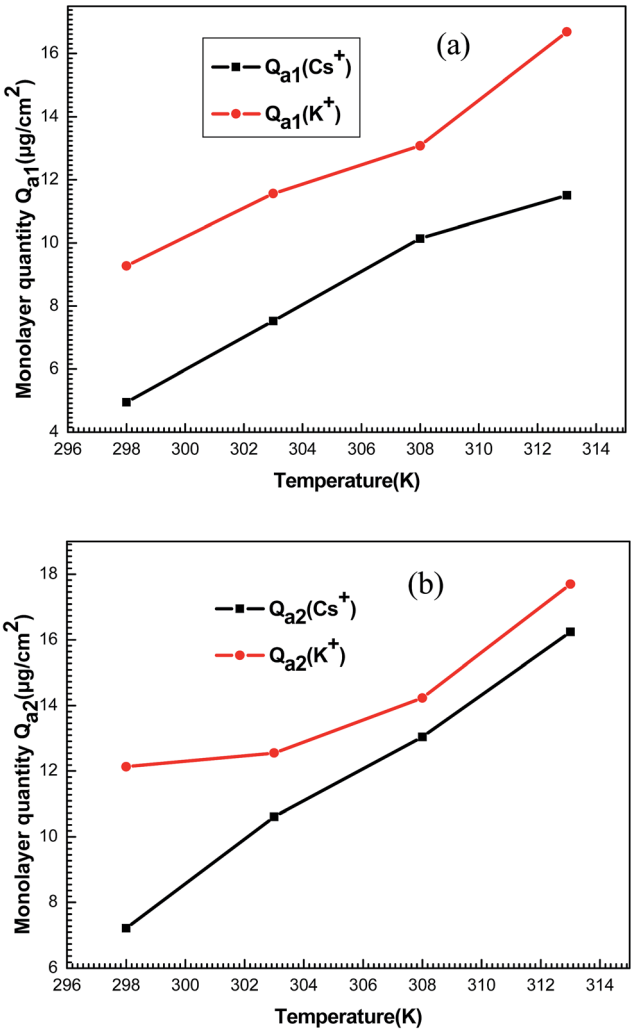

Fig. 12 Behavior of monolayer adsorbed quantities Q_{a1} (a) and Q_{a2} (b) of potassium and cesium ions as a function of temperature.

4.1.3. Monolayer adsorbed quantities Q_{a1} and Q_{a2}. The amounts of adsorbed monolayer Q_{a1} and Q_{a2} indicate the quantity of potassium or cesium adsorbed at first layer. These adsorbed quantities at saturation are related to n_1, n_2 and N_{M1}, N_{M2} by the relations: $Q_{a1} = n_1{*}N_{M1}$ and $Q_{a2} = n_2{*}N_{M2}$. The variations of these parameters for the two systems are given in Fig. 12.

It can be seen that the values increased with increased temperature. This behavior is not seen commonly and it can be explained using the correlation of the steric parameters (n_1, n_2, N_{M1} and N_{M2}). Aforementioned, the numbers of ions on per site and the densities of receptor sites increased depending on the temperature. Consequently, the behavior of these steric parameters led to the increase of the monolayer adsorbed quantities with the temperature.

The adsorption process is governed by the previous parameters. Nevertheless, these parameters cannot explain the decrease of adsorbed quantities after partial saturation. Then, the energetic parameters c_1 and c_2 can explain this behavior. Therefore, the adsorption energies constitute a dominant factor of the adsorption process.

Table 6 Adsorption energies of (a) K^+–helicene at 298 K, 303 K, 308 K and 313 K

T (K)	$-\Delta E_1{}^a$ (kJ mol^{-1})	$-\Delta E_2{}^a$ (kJ mol^{-1})
298	−35.66	−25.96
303	−35.70	−25.21
308	−36.09	−25.80
313	−36.58	−26.59

4.2. Energetic interpretations and adsorption energies

In general, the adsorption process is controlled by the adsorption energy. The molar adsorption energies ($-\Delta E_1{}^a$) and ($-\Delta E_2{}^a$) characterize the interactions between the adsorbate ions and the adsorbent surface. Using the values of the parameters w_1 and w_2 given in eqn (23) and (24) the adsorption energies can be written as:

$$-\Delta E_1{}^a = RT \ln(w_1/c_{si}) \quad (25)$$

$$-\Delta E_2{}^a = RT \ln(w_2/c_{si}) \quad (26)$$

where c_{si} is the solubility of potassium or cesium ions.

According to the literature, the type of interaction can be classified, to a certain extent, by the magnitude of the change in adsorption energy. Physical adsorptions such as hydrogen bonding or van der Waals forces usually prove energies values $|\Delta E^a| < 30$ kJ mol^{-1}.[40,41] Other physical adsorption mechanisms such as electrostatic interactions were between 10 and 50 kJ mol^{-1}.[42] Whereas, chemical adsorptions such as covalent binding force or ionic link are usually $|\Delta E^a| > 80$ kJ mol^{-1}.[47] The calculated adsorption energies are illustrated in Tables 6 and 7.

One can note that the different values of the adsorption energies $|\Delta E^a|$ are <40 kJ mol^{-1}, which imply that the adsorption of K^+ and Cs^+ ions on hepta-helicenes take place *via* physical adsorption such binding is electrostatic interactions. These findings are agree with the work elaborated by Tan *et al.*[43] and Tsuzuki *et al.*[44] which suggest that the interaction of [7]-helicene with alkali cations brings in the important problem of cation–π interactions[43–46] constitute a general non-covalent binding force. So, the alkali metals are physisorbed onto the adsorbent helicenes.

It is also noted that the adsorption energies of K^+ are superior to Cs^+ which imply that K^+–helicene is more stable than the complex Cs^+–helicene. Such proposition is agree with the work of Saini *et al.*[47] which elucidate that the helicene can be used as a biosensor of K^+ and Cs^+ with same order of stability.

Table 7 Adsorption energies of (b) Cs^+–helicene at 298 K, 303 K, 308 K and 313 K

T (K)	$-\Delta E_1{}^a$ (kJ mol^{-1})	$-\Delta E_2{}^a$ (kJ mol^{-1})
298	−33.02	−23.05
303	−33.29	−23.31
308	−34.13	−24.04
313	−35.01	−24.67

5. Conclusion

The adsorption of potassium and cesium ions onto hepta-Helicens molecules was studied by the grand canonical ensemble in statistical physics, to find new microscopic interpretations. The adsorption measurements have been carried out using a quartz crystal microbalance. A new statistical model with two energies was developed and applied for these systems. It was found that the proposed statistical treatment is sufficiently flexible to give a good representation of experimental data. Some physicochemical parameters related to the adsorption process were introduced in the analytical model expression and they were directly obtained from the fitting of the experimental adsorption isotherms by numerical simulation.

These parameters are divided into two types. The first type of parameters contains four main parameters, namely the number of ions per site, n_1 and n_2, and the densities of receptor sites N_{M1} as well as N_{M2}. The second type of parameters is mainly the two energetic parameters c_1 and c_2 which respectively referred to the concentrations at half saturations.

The fitting values of n_1 and n_2 show that the numbers of adsorbed ions K^+ and Cs^+ increased with the temperature which is due to the thermal agitation effect. The study of the density of receptor sites N_{M1} and N_{M2} indicates that when the temperature increases new hidden sites appear and participate in the adsorption which leads to an increase in the amount of adsorbed ions. The values of the adsorption energies obtained through the model indicated that both adsorptions processes were typical of a physisorption which electrostatic interactions are involved, the [7]-helicene could function as potassium and cesium sensor and the K^+–helicene complex is more stable than the Cs^+–helicene complex.

Conflicts of interest

There are no conflicts to declare.

References

1 Y. Shen and C. F. Chen, *Chem. Rev.*, 2012, **112**, 1463.
2 M. Gingras, *Chem. Soc. Rev.*, 2013, **42**, 968.
3 F. Torricelli, J. Bosson, C. Besnard, M. Chekini, T. Burgi and J. Lacour, *Angew. Chem., Int. Ed.*, 2013, **52**, 1796.
4 Y. Nakai, T. Mori and Y. Inoue, *J. Phys. Chem. A*, 2013, **117**, 83.
5 M. J. Fuchter, J. Schaefer, D. K. Judge, B. Wardzinski, M. Weimar and I. Krossing, *Dalton Trans.*, 2012, **41**, 8238.
6 K. Nakano, H. Oyama, Y. Nishimura, S. Nakasako and K. Nozaki, *Angew. Chem., Int. Ed.*, 2012, **51**, 695.
7 T. J. Katz and J. Pesti, *J. Am. Chem. Soc.*, 1982, **104**, 346.
8 A. Sudhakar and T. J. Katz, *J. Am. Chem. Soc.*, 1986, **108**, 179.
9 J. Bosson, J. Gouin and J. Lacour, *Chem. Soc. Rev.*, 2014, **43**, 2824.
10 Y. Xu, Y. X. Zhang, H. Sugiyama, T. Umano, H. Osuga and K. Tanaka, *J. Am. Chem. Soc.*, 2004, **126**, 6566.
11 D. Z. G. Wang and T. J. Katz, *J. Org. Chem.*, 2005, **70**, 8497.
12 N. Takenaka, J. Chen, B. Captain, R. S. Sarangthem and A. Chandrakumar, *J. Am. Chem. Soc.*, 2010, **132**, 4536–4537.
13 I. Sato, R. Yamashima, K. Kadowaki, J. Yamamoto, T. Shibata and K. Soai, *Angew. Chem., Int. Ed.*, 2001, **40**, 1096.
14 F. G. Klärner and B. Kahlert, *Acc. Chem. Res.*, 2003, **36**, 919.
15 M. Harmata, *Acc. Chem. Res.*, 2004, **37**, 862.
16 C. W. Chen and H. W. Whitlock Jr, *J. Am. Chem. Soc.*, 1978, **100**, 4921.
17 M. P. Johansson and M. Patzschke, *Chem.–Eur. J.*, 2009, **15**, 13210.
18 R. H. Janke, G. Haufe, E. U. Würthwein and J. H. Borkent, *J. Am. Chem. Soc.*, 1996, **118**, 6031.
19 S. Grimme and S. D. Peyerimhoff, *J. Chem. Phys.*, 1996, **204**, 411.
20 J. M. Schulman and R. L. Disch, *J. Phys. Chem. A*, 1999, **103**, 6669.
21 H. M. Sobell, Actinomycin and DNA transcription, *Proc. Natl. Acad. Sci. U. S. A.*, 1985, **82**, 5328–5331.
22 G. Sener, E. Ozgur, E. Yılmaz, L. Uzun, R. Say and A. Denizli, *Biosens. Bioelectron.*, 2010, **26**, 815.
23 J. Rickert, T. Weiss, W. Kraas, G. Jung and W. Göpel, *Biosens. Bioelectron.*, 1996, **11**, 591.
24 C. K. O'Sullivan and G. G. Guilbault, *Biosens. Bioelectron.*, 1999, **14**, 663.
25 T. Nomura and M. Okuhara, *Anal. Chim. Acta*, 1982, **142**, 281.
26 K. Park, M. Koh, C. Yoon and H. H. Kim, *J. Supercrit. Fluids*, 2004, **29**, 203.
27 P. Skládal, *J. Braz. Chem. Soc.*, 2003, **14**, 1678.
28 A. J. Bard and C. G. Zoski, *Electroanalytical Chemistry: A Series of Advances*, CRC PressTaylor & Francis Group, USA, 2013.
29 S. Knani, M. Mathlouthi and A. Ben Lamine, *Food Biophys.*, 2007, **2**, 183.
30 M. Ben Yahia, L. B. H. Hsan, S. Knani, M. Ben Yahia, H. Nasri and A. B. Lamine, *J. Mol. Liq.*, 2016, **222**, 576.
31 B. Diu, C. Guthmann, D. Lederer and B. Roulet, *Physique Statistique*, Hermann, Paris, 1989.
32 S. Knani, F. Aouaini, N. Bahloul, M. Khalfaoui, M. A. Hachicha, A. Ben Lamine and N. Kechaou, *Phys. A*, 2014, **400**, 57.
33 M. Ben Yahia, F. Aouaini, M. A. Hachicha, S. Knani, M. Khalfaoui and A. Ben Lamine, *Phys. B*, 2013, **419**, 100.
34 L. Sellaoui, S. Knani, A. Erto, M. A. Hachicha and A. Ben Lamine, *Fluid Phase Equilib.*, 2016, **408**, 259.
35 F. Aouaini, S. Knani, M. Ben Yahia, N. Bahloul, N. Kechaou and A. Ben Lamine, *Drying Technol.*, 2014, **32**, 1905.
36 D. W. Marquardt, *J. Soc. Ind. Appl. Math.*, 1963, **11**, 431.
37 A. Nakhli, M. Bergaoui, M. Khalfaoui, J. Mollmer, A. Moller and A. Ben Lamine, *Adsorption*, 2014, **20**, 987.
38 S. Knani, M. Khalfaoui, M. A. Hachicha, A. Ben Lamine and M. Mathlouthi, *Food Chem.*, 2012, **132**, 1686.
39 G. L. Dotto, L. A. Pinto, M. A. Hachicha and S. Knani, *Food Chem.*, 2015, **171**, 1.
40 B. von Oepen, W. Kördel and W. Klein, *Chemosphere*, 1991, **22**, 285.
41 C. Ye, N. Hu and Z. Wang, *J. Taiwan Inst. Chem. Eng.*, 2012, **44**, 74.
42 Y. Wang, Y. Qi, Y. Li, J. Wu, X. Ma, C. Yu and L. Ji, *J. Hazard. Mater.*, 2013, **260**, 9.

43 X. J. Tan, W. L. Zhu, M. Cui, X. M. Luo, J. D. Gu, I. Silman, J. L. Sussman, H. L. Jiang, R. Y. Ji and K. X. Chen, *J. Phys. Chem. Lett.*, 2001, **349**, 113.
44 S. Tsuzuki, M. Yoshida, T. Uchimaru and M. Mikami, *J. Phys. Chem. A*, 2001, **105**, 769.
45 J. C. Ma and D. A. Dougherty, *Chem. Rev.*, 1997, **97**, 1303.
46 J. Sunner, K. Nishizawa and P. Kebarle, *J. Phys. Chem.*, 1981, **85**, 1814.
47 S. Saini and B. M. Deb, *Indian J. Chem., Sect. A: Inorg., Bio-inorg., Phys., Theor. Anal. Chem.*, 2007, **46**, 9.